110-GHz f_T Silicon Bipolar Transistors Implemented Using Fluorine Implantation for Boron Diffusion Suppression

M. N. Kham, H. A. W. El Mubarek, J. M. Bonar, Peter Ashburn, *Member, IEEE*, P. Ward, L. Fiore, R. Petralia, C. Alemanni, and A. Messina

***Abstract*—This paper investigates how fluorine implantation can be used to suppress boron diffusion in the base of a double polysilicon silicon bipolar transistor and hence deliver a record f_T of 110 GHz. Secondary ion mass spectroscopy (SIMS) and transmission electron microscopy (TEM) are used to characterize the effect of the fluorine implantation energy and dose, the anneal temperature and the germanium pre-amorphization implant on the fluorine profiles. These results show that retention of fluorine in the silicon is maximized when a high-energy fluorine implant is combined with a low thermal budget inert anneal. TEM images show that a high-energy fluorine implant into germanium pre-amorphized silicon eliminates the end of range defects from the germanium implant and produces a band of dislocation loops deeper in the silicon at the range of the fluorine implant. Boron SIMS profiles show a suppression of boron diffusion for fluorine doses at and above 5×10^{14} cm^{-2}, but no suppression at lower fluorine doses. This suppression of boron diffusion correlates with the appearance on the SIMS profiles of a fluorine peak at a depth of approximately $R_p/2$, which is attributed to fluorine trapped in vacancy–fluorine clusters. The introduction of a fluorine implant at this critical fluorine dose into a bipolar transistor process flow leads to an increase in cutoff frequency from 46 to 60 GHz. Further optimization of the base-width and the collector profile leads to a further increase in cutoff frequency to 110 GHz. Two factors are postulated to contribute to the suppression of boron diffusion by the fluorine implant. First, the elimination of the germanium end of range defects, and the associated interstitial population, by the fluorine implant, removes a source of transient enhanced diffusion. Second, any interstitials released by the dislocation loops at the range of the fluorine implant would be expected to recombine at the vacancy–fluorine clusters before reaching the boron profile.**

***Index Terms*—Bipolar transistor, diffusion, fluorine, silicon, transient enhanced diffusion.**

I. Introduction

OVER THE past few years there has been considerable interest in the behavior of fluorine in silicon for application in both bipolar and MOS devices. This interest was initially stimulated by the use of a BF_2^+ implant for shallow p-n junction formation [1], but more recently by the effect of fluorine on boron diffusion [2]. Initial work gave conflicting results for the effects of fluorine on boron diffusion, with some research showing that fluorine had little or no effect on boron diffusion [3] and other research showing complete suppression of boron transient enhanced diffusion (TED) [4]–[6] and also increased boron activation [2]. These contradictory results have been reconciled by careful analysis of the experimental conditions used for the fluorine and boron implants. For example, for boron implants into pre-amorphized silicon, it has been shown that fluorine dramatically increases boron diffusivity in the early stages of the anneal due to the reduction of the dangling bond concentration in the amorphous silicon by the fluorine [3]. Also the fluorine dose and energy have a strong effect on the degree that the boron diffusivity is suppressed. For example, low dose fluorine implants give reduced boron TED, whereas high dose fluorine implants also give reduced boron thermal diffusion by a factor of four [8].

For fluorine implants into crystalline silicon, research has shown that the mechanism by which fluorine suppresses boron diffusion is different for boron TED and boron thermal diffusion [8], [9]. The reduction of boron thermal diffusion correlates with the presence of a shallow fluorine peak at a depth of approximately $R_p/2$, where R_p is the projected range of the fluorine implant. It has been proposed that the $R_p/2$ peak is due to self vacancy–fluorine clusters [8], [10], and that the clusters suppress the self interstitial concentration in the vicinity of the boron profile and hence reduce boron thermal diffusion. In contrast, the suppression of boron TED correlates with the presence of a band of dislocation loops at approximately the range, R_p, of the fluorine implant [9]. It has been proposed that the suppression of boron TED is then explained by the retention of self interstitials in the dislocation loops, which suppresses their backflow to the surface. The effect of fluorine in silicon pre-amorphized using a silicon implant has also been researched and similar suppressions of boron TED and thermal diffusion seen [11], [12]. Impellizzeri *et al.* [11] proposed that the presence of fluorine during the solid phase epitaxy (SPE) of MBE material leads to a vacancy–rich silicon layer through the formation of vacancy–fluorine clusters. Upon post-SPE annealing, the self-interstitials released from end-of-range defects are annihilated by the vacancy–fluorine clusters, thereby reducing the flux of back diffusing interstitials to the surface. A similar mechanism has been used to explain the reduction in boron de-activation in ultrashallow junctions by the presence of fluorine [12].

Manuscript received July 6, 2005; revised December 8, 2005. This work was supported in part by EPSRC and IST 30132, and in part by PERLA. The work of H. A. W. El Mubarek was supported by Royal Academy of Engineering and the Engineering and Physical Sciences Research Council (EPSRC) for the award of a fellowship. The review of this paper was arranged by Editor J. Burghartz.

M. N. Kham, H. A. W. El Mubarek, J. M. Bonar, and P. Ashburn are with the School of Electronics and Computer Science, University of Southampton, Southampton SO17 1BJ, U.K.

P. Ward is with STMicroelectronics, Sicily, Italy, and also with PWCE Consulting.

L. Fiore, R. Petralia, C. Alemanni, and A. Messina are with STMicroelectronics, Sicily, Italy.

Digital Object Identifier 10.1109/TED.2005.864368

Recently fluorine implantation has been applied to MOS transistors to reduce boron diffusion in critical areas of the source and drain [13], [14]. Liu *et al.* [13] used a 1×10^{15} cm^{-2} fluorine implant to create a super halo for both 50-nm n- and p-channel transistors. The fluorine-assisted halo process resulted in reduced junction capacitance and an improved $I_{\rm on}$-$I_{\rm off}$ tradeoff. Fukutome *et al.* [14] used a 5×10^{14}–2×10^{15} cm^{-2} fluorine implant prior to the p-channel extension implant to minimize the diffusion of boron in the extension. The fluorine implant led to dramatically improved threshold voltage roll-off characteristics without any degradation of drive current in sub50 nm p-channel MOSFETs. Scanning tunnelling microscopy was used to show that the improvement was due to a reduction of the overlap length, for example from 13 to 7 nm in 40-nm gate length p-channel MOSFETs.

While fluorine implantation is increasingly being applied to MOS transistors, to date no work has been reported on the application of fluorine to silicon bipolar transistors. In this paper, we therefore investigate the use of fluorine implantation to suppress boron diffusion in the base of silicon bipolar transistors. We begin by discussing the main process variables that can be used to optimize the effect of the fluorine and hence implement fluorine implantation in a production silicon bipolar technology. We show that the fluorine implant dramatically suppresses boron diffusion in the base and leads to a value of Ft as high as 110 GHz in an appropriately optimized device.

II. Experimental Procedure

To investigate the main process variables that influence the fluorine profiles, silicon (100) wafers were implanted with fluorine at energies of 50 and 185 keV. The doses of the 50-keV (1×10^{15} cm^{-2}) and 185-keV (2×10^{15} cm^{-2}) implants were adjusted to give the same peak fluorine concentration of around 8×10^{19} cm^{-3}. To investigate the effect of pre-amorphization, some wafers were implanted with 80-keV, 1×10^{15} cm^{-2} Ge^{+} prior to fluorine implant. In the initial experiments, the boron base was fabricated using a 22-keV BF_2^+ implant (equivalent to a 5-keV B^+ implant). In later transistor optimization experiments, a thinner base was fabricated using a 14-keV BF_2^+ implant (equivalent to a 3-keV B^+ implant). The implantation anneals were carried out using rapid thermal annealing at temperatures in the range 900 °C–1025 °C.

The baseline transistors studied in this paper were fabricated using a 0.25-μm double polysilicon bipolar technology. The base was fabricated using a 80-keV, 1×10^{15} cm^{-2} germanium pre-amorphization implant, a 5-keV base implant and a Solid Phase Epitaxy (SPE) anneal at 700 °C to recrystallise the amorphized silicon. After base formation, the transistors received additional thermal treatments arising from the deposition of a vapox layer, a short RTA vapox densification, the deposition of nitride spacers at 850 °C for 90 min, the deposition of the LPCVD polysilicon emitter and the final rapid thermal anneal of 10 s in nitrogen at 1000 °C. In the fluorine-enriched transistors, the fluorine implant was inserted after the germanium pre-amorphization implant but before the base implantation and SPE anneal; here the vapox densification was omitted.

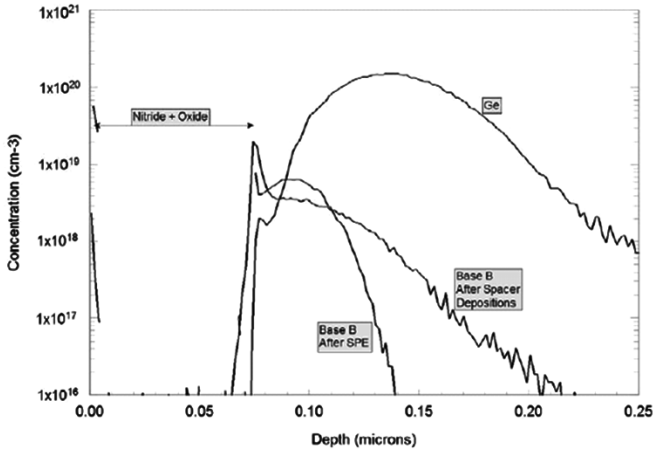

Fig. 1. Boron SIMS profiles for the baseline double polysilicon silicon bipolar technology after the 700 °C solid phase epitaxy anneal and after the 90 min nitride spacer deposition. The germanium profile for the germanium pre-amorphization implant is also shown for comparison.

Boron (B11) and fluorine (F19) concentration depth profiles were obtained on all samples by secondary ion mass spectroscopy (SIMS) using a 5-keV oxygen beam with oxygen flooding. The annealed boron SIMS profiles were fitted using the Fermi diffusion model in the Silvaco Athena simulation program and the diffusion coefficient was extracted from the best fit obtained. The layers were also analyzed by transmission electron microscopy (TEM).

III. Results

Fig. 1 shows SIMS boron profiles for the baseline transistors at different stages of the double polysilicon bipolar process. Also included is a germanium profile used for the pre-amorphization implant after completion of the device processing; it should be noted that Ge diffusion is minimal for all the process conditions used. The boron profile after SPE anneal is very sharp and gives a junction depth, at a collector concentration of 1×10^{17} cm^{-3}, of 0.052 μm; this collector concentration is typical of that used for these high frequency transistors (see Fig. 9). However, the additional thermal treatments required to fabricate the self-aligned polysilicon emitter structure (vapox deposition and densification and nitride spacer deposition at 850 °C for 90 min) lead to broadening of the boron profile, typical of TED, so that at the end of the process the junction depth has increased to 0.090 μm. This increase in the width of the boron profile during polysilicon emitter processing is addressed below using a fluorine implant to suppress the boron diffusion and hence avoid the inherent loss of RF performance. It should be noted that all the experiments relating to transistor structures use low oxygen and carbon CVD epitaxial silicon layers in order avoid interference in the results by those elements.

A. Analysis of Fluorine Profiles

The results of an investigation of the sensitivity of the fluorine profile to the implant energy are shown in Fig. 2, which presents fluorine profiles for 185-keV (Fig. 2(a)) and 50-keV [Fig. 2(b)] F^+ implants into crystalline silicon after a 60-s anneal at 900 °C. For the 185-keV fluorine profile a deep peak is present around

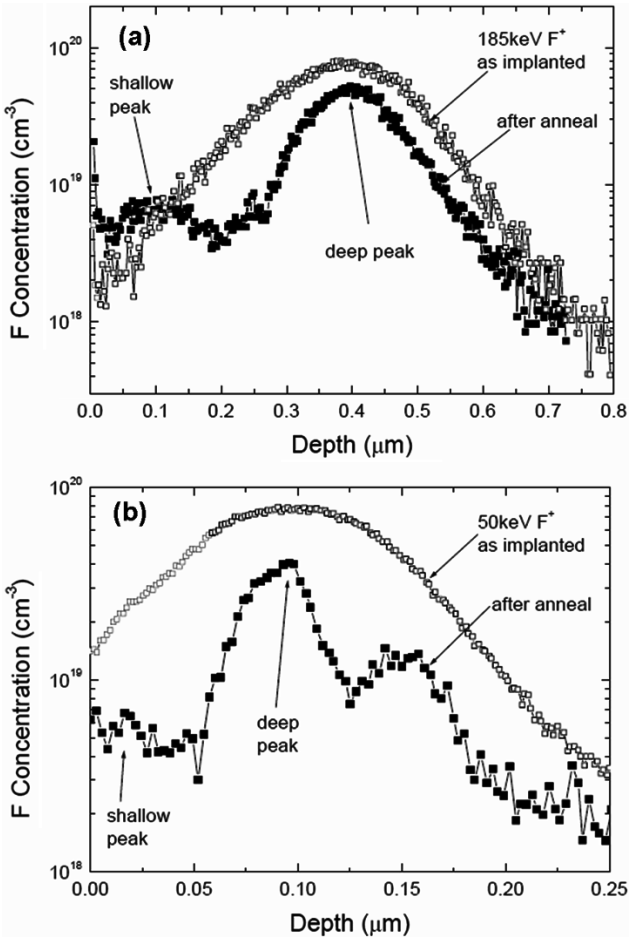

Fig. 2. SIMS profiles for 185- and 50-keV F^+ implants into crystalline silicon after implant and after a 60-s anneal at 900 °C.

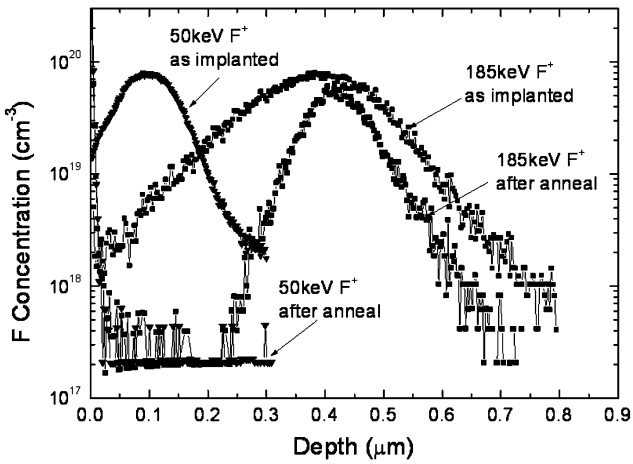

Fig. 3. SIMS profiles for 185- and 50-keV F^+ implants into crystalline silicon after implant and after a 60-s anneal at 1000 °C.

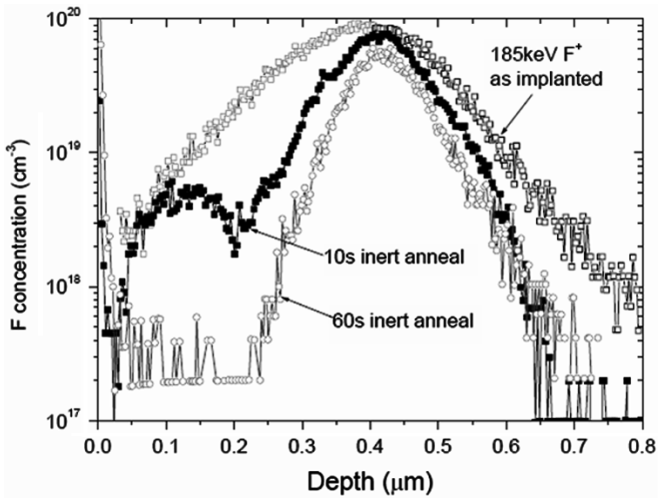

Fig. 4. SIMS profiles for a 185-keV F^+ implant into crystalline silicon, after implant and after 10 and 60-s inert anneal at 1000 °C.

the projected range, R_p, of the fluorine implant and a shallow peak is present at a depth of $0.25R_p$ (0.10 μm), extending to a depth of about $R_p/2$ (0.21 μm). It has been shown that the R_p peak is due to fluorine trapped at dislocation loops and it has been proposed that the $R_p/2$ peak is due to fluorine trapped in vacancy–fluorine clusters [8], [10]. For fluorine implants into crystalline silicon, the $R_p/2$ peak correlates with a suppression of boron thermal diffusion [8] and the R_p peak correlates with a suppression of boron TED [9]. An equivalent pair of peaks is seen in Fig. 2 for the 50-keV F^+ implant. The deep fluorine peak is present at a depth of approximately 0.10 μm and the shallow peak is present at a depth of 0.02 μm ($0.20R_p$), extending to a depth of approximately 0.05 μm ($R_p/2$). These results suggest that the deep dislocation loops and the shallow vacancy–fluorine clusters are formed for both 185- and 50-keV F^+ implants, and hence the fluorine profiles are not highly sensitive to the choice of fluorine energy.

The results of an experiment to investigate the role of anneal temperature on the fluorine profiles are shown in Fig. 3, which presents fluorine profiles for 185- and 50-keV F^+ implants into crystalline silicon after a 60-s anneal at 1000 °C. At this temperature, the SIMS profiles show considerable loss of fluorine from the sample during the anneal; for the 185-keV F^+ implant, the deep peak is present but the shallow peak is absent, whereas for the 50-keV F^+ implant there is little fluorine remaining in the sample. These results imply that both the vacancy–fluorine clusters and the dislocation loops can be dissolved if an extended anneal at a high temperature is carried out.

The results of an experiment to investigate the effect of anneal time on the fluorine profiles are shown in Fig. 4, which presents fluorine profiles for a 185-keV F^+ implant into crystalline silicon, followed by a 10-s or 60-s anneal at 1000 °C in an inert ambient. For the 10-s anneal, the deep fluorine peak is present at a depth of approximately 0.42 μm and the shallow peak is present at a depth of $0.29R_p$ (0.12 μm), extending to a depth of approximately $R_p/2$ (0.2 μm). In contrast for the 60-s anneal, the deep fluorine peak is present, but the shallow fluorine peak is absent. These results indicate that a 60-s anneal at 1000 °C is sufficient to dissolve the vacancy–fluorine clusters.

Pre-amorphization prior to boron base implantation is desirable in bipolar technology to eliminate the implantation-induced, planar scattering, channelling tail on the boron profile. The results of an experiment to investigate the effect of a germanium pre-amorphization implant on the fluorine profiles are shown in Fig. 5, which presents fluorine profiles for samples given a germanium pre-amorphization implant and

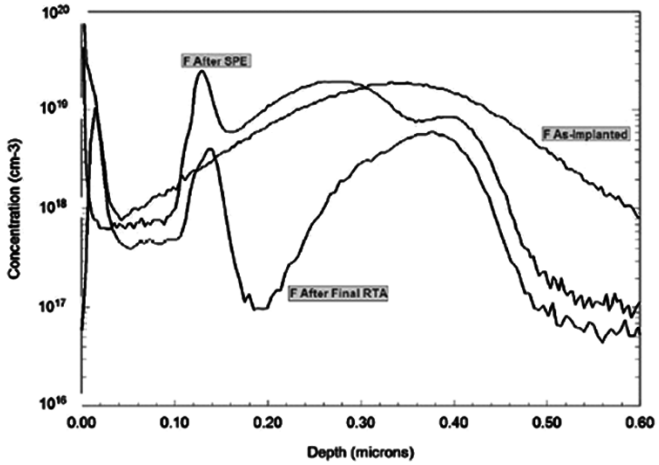

Fig. 5. SIMS profiles for samples given a germanium pre-amorphization implant and a 150-keV F^+ implant at 5×10^{14} cm^{-2}. One sample was given all the thermal treatments needed to produce a double polysilicon emitter bipolar transistor, including solid phase epitaxy anneal, a vapox deposition and densification, a nitride spacer deposition of 90 min at 850 °C and a final anneal of 10-s in N_2 at 1000 °C. The second sample only received the SPE anneal of 300 s at 700 °C.

a 150-keV F^+ implant at 5×10^{14} cm^{-2}. One sample was given all the thermal treatments needed to produce a double polysilicon emitter bipolar transistor mentioned in Section 2, including a final anneal of 10 s in N_2 at 1000 °C. The second sample only received the SPE anneal of 300 s at 700 °C. The fluorine profile after final RTA shows similar key features as the 10-s anneal profile in Fig. 4 for a fluorine implant into crystalline silicon. A deep peak can be seen at a depth of about 0.37 μm ($1.1R_p$) and a shallow peak at a depth of 0.14 μm ($0.39R_p$), extending to a depth of about 0.18 μm ($R_p/2$). There is also an elevated fluorine concentration of 4–5 $\times 10^{17}$ cm^{-3} extending from the shallow fluorine peak to the silicon surface. The fluorine peak at the surface is a measurement artefact due to the spacer surface layers trapping fluorine and ion beam mixing effects during analysis. The fluorine profile after the 700 °C SPE anneal shows much higher levels of fluorine retention in the sample, particularly at depths between about 0.13 and 0.36 μm, perhaps due to some remaining microscopic crystal damage. The shallow fluorine peak can be clearly seen at a depth of 0.13 μm and two deeper peaks at depths of 0.27 and 0.39 μm. It is interesting to note that considerable fluorine diffusion has occurred during the SPE anneal, even though the thermal budget of 300 s at 700 °C was very light. This result is consistent with the fast diffusion of fluorine that has been reported in amorphous silicon [16].

Fig. 6 presents cross-section TEM micrographs for samples without (Fig. 6(a)) and with (Fig. 6(b)) a 5×10^{14} cm^{-2} 150-keV fluorine implant after the SPE anneal. Fig. 6(a) shows that the pre-amorphized silicon layer has recrystallised during the SPE anneal, leaving a line of defects centred at a depth of about 0.12 μm; this depth closely corresponds to the thickness of the amorphous silicon layer created by the germanium implant, and hence it can be concluded that these are the conventional "end of range defects" due to the precipitation of an excess of self interstitials. In contrast, the fluorine implanted sample in Fig. 6(b) shows a line of dislocation loops much deeper in the sample,

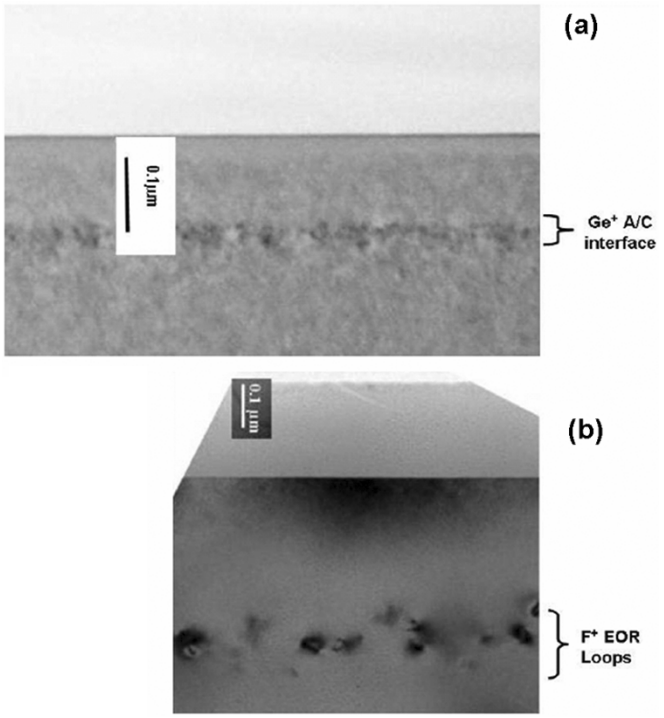

Fig. 6. Cross section TEM micrographs for samples (a) without and (b) with a 5×10^{14} cm^{-2} 150-keV fluorine implant after the SPE anneal. The magnification bar is 0.1 μm in both cases.

centred at the range of the fluorine implant (0.37 μm); there is no evidence of end of range defects created by the germanium implant at a depth of 0.12 μm.

B. Effect of Fluorine on Boron Base Profile

In this section, we consider how a fluorine implant can be used to minimize boron diffusion in the base and, hence, how a scaled basewidth can be produced. Fig. 7 shows boron and fluorine SIMS profiles (oxygen beam) for transistor structures implanted with germanium for pre-amorphization, with different doses of fluorine at 150 keV and with a 14-keV BF_2^+ base implant. The wafers received all the thermal treatments needed to produce a double polysilicon emitter bipolar transistor except the vapox anneal. For the low fluorine dose results in Fig. 7(a) the final rapid thermal anneal was also omitted, whereas for the high fluorine dose results in Fig. 7(b), a comparison is made of profiles with and without the final rapid thermal anneal. For fluorine doses of 1 and 2×10^{14} cm^{-2} in Fig. 7(a), a sharp fluorine peak can be seen at the polysilicon/silicon interface, but no $R_p/2$ fluorine peak is present. The deep fluorine peak at the range of the fluorine implant was also present, but is not shown in Fig. 7(a) for the sake of clarity. The boron profiles in Fig. 7(a) are reasonably broad, giving junction depths of 0.103 and 0.108 μm, respectively, at collector doping concentrations of 1×10^{17} cm^{-3}. These boron profiles show the presence of significant boron diffusion during the 90 min at 850 °C nitride spacer deposition. In contrast, for a fluorine dose of 5×10^{14} cm^{-2}, Fig. 7(b) shows that the $R_p/2$ fluorine peak is now present both after the nitride spacer deposition and after the final rapid thermal anneal. Furthermore, the boron profile is much sharper and does not change with the final rapid thermal

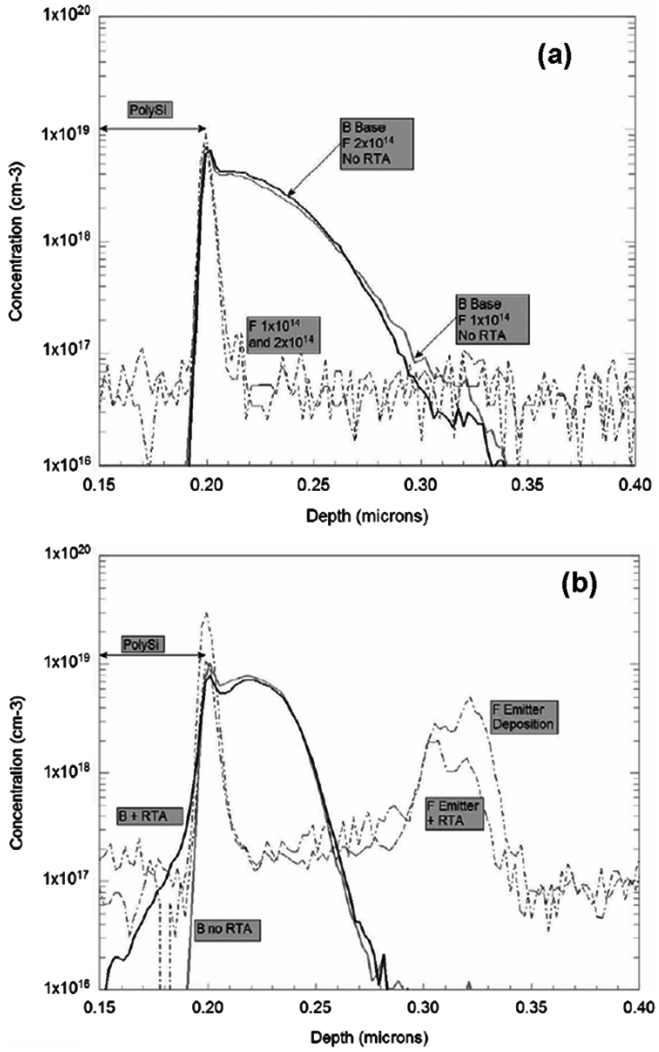

Fig. 7. Boron and fluorine SIMS profiles (oxygen beam) for transistor structures implanted with germanium for pre-amorphization, with different doses of fluorine at 150 keV and with a 14-keV BF_2^+ base implant. The wafers received all the thermal treatments needed to produce a double polysilicon emitter bipolar transistor except the vapox anneal. For the low fluorine dose results (a) the final rapid thermal anneal was also omitted, whereas for the high fluorine dose results (b) a comparison is made of profiles with and without the final rapid thermal anneal.

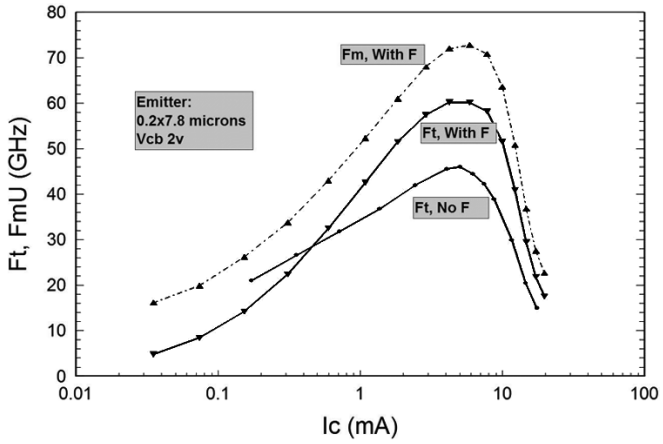

Fig. 8. Graph of F_t and F_m as a function of collector current for the baseline double polysilicon silicon bipolar process (22-keV BF_2^+ base implant) and a graph of F_t as a function of collector current for an analogous process with a 150-keV, 5×10^{14} cm^{-2} F^+ implant. The two types of transistor received the same thermal budgets, with the exception of the vapox densification, which was omitted for the transistor implanted with fluorine.

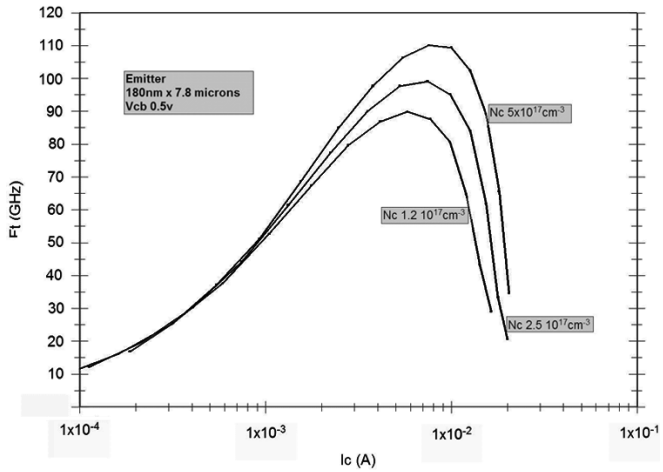

Fig. 9. Graph of F_t as a function of collector current for a double polysilicon silicon bipolar process (14-keV BF_2^+ base implant) with a 150-keV, 5×10^{14} cm^{-2} F^+ implant and for three different collector doping concentrations.

anneal. At a doping concentration of 1×10^{17} cm^{-3}, the junction depth is 0.070 μm. These results show that a critical fluorine dose of 2–5 $\times 10^{14}$ cm^{-2} exists, above which a significant suppression of boron diffusion is obtained and below which the fluorine has no effect. Furthermore, this critical fluorine dose for boron diffusion suppression correlates with the appearance of the $R_p/2$ fluorine peak on the SIMS profile. The separate SIMS profile (Cs beam) for the deep *F* peak has been shown already in Fig. 5 for the highest dose. Here it is clear that the R_p peak is present and that approximately 10% of the original fluorine dose is retained by the deep dislocation loops.

C. Bipolar Transistor Performance

To investigate the effectiveness of fluorine implantation for basewidth reduction, the baseline process with a 22-keV BF_2^+ base implant was used to fabricate transistors with and without a 150 keV, 5×10^{14} cm^{-2} F^+ implant. Fig. 8 shows a graph of F_t as a function of collector current, and it can be seen that the fluorine implant increases the maximum F_t from 46 to 60 GHz. For completeness Fig. 8 also shows values of $F_{\max}$ as a function of collector current for the fluorine implanted transistor and a peak $F_{\max}$ of 72 GHz is obtained.

Having demonstrated that a fluorine implant is able to dramatically improve the F_t in the baseline double polysilicon bipolar process, we then proceeded to scale the basewidth, while at the same time keeping the germanium and fluorine implants the same. A flat collector doping profile was obtained close to the base by means of implanting low doses of phosphorous at three energies; 60, 120, and 180 keV. The collector doping was then easily varied by changing the implant doses. Fig. 9 shows a graph of F_t as a function of collector current for three different values of collector doping. It can be seen that values of peak F_t of 90, 100, and 110 GHz are obtained for collector junction concentrations of 1.2, 2.5, and 5.0 $\times 10^{17}$ cm^{-2} respectively.

The value of BV_{ceo} at $\sim$5 mA collector current varied slightly with collector implant dose, with values around 2.5 V, such that all three variants had Johnson numbers of $\sim$ 250 GHz V. As far as the authors are aware, these values of F_t are the highest ever reported for silicon bipolar transistors. The Johnson numbers are comparable with SiGeC epitaxial HBTs with similar RF performance.

IV. Discussion

A comparison of the TEM cross sections in Fig. 6 with the fluorine profiles in Fig. 5 allows the fluorine profiles in the pre-amorphized samples to be interpreted. The dislocation loops in Fig. 6(b) seen after the SPE anneal lie at depths between about 0.24 and 0.46 μm, which corresponds very well with the two deep fluorine peaks in Fig. 5 at depths of 0.27 and 0.39 μm. It can therefore be concluded that these two fluorine peaks are due to fluorine trapped at the dislocation loops. For the sample without a fluorine implant in Fig. 6(a), the end of range defects created by the germanium implant lie at depths between about 0.11 and 0.15 μm, whereas for the sample with a fluorine implant in Fig. 6(b) there is no evidence of any defects at this depth. This is an interesting result and indicates that the fluorine implant has suppressed the formation of end of range defects from the germanium pre-amorphization implant and has instead created deeper-lying dislocation loops around the range of the subamorphizing fluorine implant. This suggests that the shallow bound F-self vacancy population generated by the F implant has compensated the excess self interstitial population produced by the Ge implant and the subsequent SPE process. For device applications, this mechanism is highly advantageous, since the dislocation loops lie much deeper than the end of range defects and hence are further away from the device depletion regions. Collector–base leakage currents measured on large arrays of F implanted devices at 3 V collector–base reverse bias show a leakage of $\sim$4 pA per transistor on a very consistent basis across wafers and from wafer to wafer. Without the F implant these leakage results are much less consistent.

For a fluorine implant into pre-amorphized silicon, Fig. 5 shows that the shallow fluorine peak lies at a depth of $0.39R_p$, which is slightly deeper than the equivalent peaks in Fig. 2 ($0.25R_p$ for 185-keV F^+ and $0.20R_p$ for 50-keV F^+) and Fig. 4 ($0.29R_p$ for the 10-s inert anneal) for the fluorine implants into crystalline silicon. This suggests that the shallow fluorine peak in Fig. 5 may have formed at the depth where end of range defects from the germanium implant would have been expected to form. However, the TEM cross section in Fig. 6(b) for the fluorine implanted sample shows no evidence of end of range defects at this depth. We can therefore conclude that the shallow fluorine peak in the pre-amorphized samples is due to fluorine trapped at defects too small to resolve by TEM. A similar result was obtained for fluorine implants into crystalline silicon [8] and this peak was shown to be due to vacancy–fluorine clusters [8]. Other authors [10], [11] have also proposed the presence of vacancy–fluorine clusters down to depths approaching the range of a fluorine implant. We therefore propose that the shallow fluorine peak in the pre-amorphized samples is due to vacancy–fluorine clusters. Further work is required to determine the detailed structure of the vacancy–fluorine clusters and to explain why the clusters are seen at the depth where end of range defects from the germanium implant would have been expected to form.

To quantify the magnitude of the boron diffusion suppression in the fluorine implanted sample, we have simulated the boron profile in Fig. 7(b) after a 5×10^{14} cm^{-2} F^+ implant an anneal of 90 min at 850 °C. An excellent fit to the measured profile was obtained for a boron diffusion coefficient of 1.1×10^{-16} cm^2/s. This value of diffusion coefficient compares with a value of 2.4×10^{-16} cm^2/s reported by Fair [21] for intrinsic boron diffusion in silicon at 850 °C. As our simulated diffusion coefficient is lower than the Fair value, we can conclude that the 5×10^{14} cm^{-2} F^+ implant has suppressed boron TED, and may also have given a small reduction in boron thermal diffusion. This TED suppression is consistent with the results of El Mubarek *et al.* [8], [9], who reported a suppression of boron TED for all fluorine doses down to 5×10^{14} cm^{-2} (the lowest dose studied) for fluorine implants into crystalline silicon. Similarly it is also consistent with the results of Impellizzeri *et al.* [11], who found a progressive reduction of boron TED for fluorine doses from 4×10^{14} cm^{-2} down to 7×10^{12} cm^{-2} for fluorine implants into pre-amorphized silicon.

The generally accepted model for transient enhanced diffusion of boron in pre-amorphized silicon is that it is associated with self-interstitials released by end of range damage created by the amorphising implant [19]. During anneal, it is thought that submicroscopic interstitial clusters are formed from excess interstitials and that these nucleate extended $\{311\}$ defects, which then unfault to form dislocation loops [20]. Self interstitials released during these processes either diffuse to other defects, such as dislocation loops (Ostwald ripening), or to the surface (dissolution). The diffusion of interstitials to the surface gives rise to transient enhanced diffusion in boron layers located near the surface. In the current work, most of the TED observed occurred during the long low temperature process associated with the silicon nitride deposition of 90 min at 850 °C.

The mechanism for TED suppression in our work can be understood by considering the fluorine profiles in Fig. 7, which show that the TED suppression correlates with the appearance of the shallow fluorine peak at a critical F^+ dose of 2–5 $\times$ 10^{14} cm^{-2}. As discussed above, we believe that this peak is due to fluorine trapped at vacancy–fluorine clusters [8]–[11]. Two factors could contribute to the TED suppression seen for fluorine doses above the critical dose. The vacancy–fluorine clusters in Fig. 7(b) are located beneath the boron profile, close to the site of the interstitial population and end of range damage created by the germanium implant alone; the subamorphising damage created by the fluorine implant is deeper still. Consequently the interstitial population generated by the germanium implant is eliminated by the presence of a compensating vacancy population, thereby removing a source of TED. Further, any interstitials released during the evolution of the deeper fluorine-induced damage, and diffusing toward the surface, would be expected to recombine at the vacancy–fluorine clusters before reaching the boron profile, again suppressing any TED. This latter mechanism was also proposed by Impellizzeri *et al.* [11], [18] to explain boron TED suppression by fluorine in samples pre-amor-

phized using a high energy silicon implant and by El Mubarek *et al.* [8], [9] for the suppression of boron thermal diffusion in crystalline silicon samples containing a boron marker layer.

V. Conclusion

A study has been made of the use of fluorine implantation for boron diffusion suppression in the context of a double polysilicon silicon bipolar technology. The effect of key processing variables on the fluorine profiles has been investigated and it has been shown that fluorine retention in the silicon is maximized if a high fluorine implant energy, and a low thermal budget anneal are used. The effect of a germanium pre-amorphization implant on both the fluorine profile and the defect structure has also been studied. TEM images have shown that the fluorine implant eliminates end of range defects from the germanium implant and instead creates a band of dislocation loops deeper in the silicon at the range of the fluorine implant. For device applications, this mechanism is highly advantageous, since the dislocation loops lie much deeper than the end of range defects and, hence, are further away from the device depletion regions. A critical fluorine dose has been identified, above which the fluorine suppresses boron diffusion and below which it has no effect. This suppression of boron diffusion correlates with the appearance of a shallow fluorine peak on the SIMS profiles at a depth of approximately $R_p/2$, and we propose that this peak is due to vacancy–fluorine clusters. Simulation of the measured boron profiles has shown that the reduced boron diffusion in the current work is primarily due to TED suppression and two factors are considered to contribute to the suppressed TED. First the elimination of the germanium end of range defects and the associated interstitial population by the fluorine implant removes a source of TED. Second, any interstitials released by the dislocation loops at the range of the fluorine implant would be expected to recombine at the vacancy–fluorine clusters before reaching the boron profile, which is located close to the silicon surface. The inclusion of a critical dose fluorine implant into the process flow of a double polysilicon silicon bipolar transistor increases the cutoff frequency from 46 to 60 GHz. Additional optimization of the base and collector profiles leads to a further increase in cutoff frequency to 110 GHz.

References

[1] R. G. Wilson, "Boron, fluorine and carrier profiles for B and BF_2 implants into crystalline and amorphous Si," *J. Appl. Phys.*, vol. 54, pp. 6879–6889, 1983.

[2] K. Ohyu, T. Itoga, and N. Natsuaki, "Advantages of fluorine introduction in boron implanted shallow p+/n junction formation," *Jpn. J. Appl. Phys.*, vol. 29, pp. 457–462, 1990.

[3] J. M. Jacques, L. S. Robertson, K. S. Jones, M. E. Law, M. Rendon, and J. Bennett, "Fluorine enhanced boron diffusion in amorphous silicon," *Appl. Phys. Lett.*, vol. 82, pp. 3469–3471, 2003.

[4] D. Fan, J. M. Parks, and R. J. Jaccodine, "Effect of fluorine on the diffusion of through-oxide implanted boron in silicon," *Appl. Phys. Lett.*, vol. 59, pp. 1212–1214, 1991.

[5] L. Y. Krasnobaev, N. M. Omelyanovskaya, and V. V. Makarov, "The effect of fluorine on the redistribution of boron in ion implanted silicon," *J. Appl. Phys.*, vol. 74, pp. 6020–6022, 1993.

[6] T. H. Huang, H. Kinoshita, and D. L. Kwong, "Influence of fluorine preamorphization on the diffusion and activation of low energy implanted boron during rapid thermal annealing," *Appl. Phys. Lett.*, vol. 65, pp. 1829–1831, 1994.

[7] D. F. Downey, J. W. Chow, E. Ishida, and K. S. Jones, "Effect of fluorine on the diffusion of boron in ion implanted silicon," *Appl. Phys. Lett.*, vol. 73, pp. 1263–1265, 1998.

[8] H. A. W. El Mubarek, M. Karunaratne, J. M. Bonar, G. D. Dilliway, Y. Wang, R. Price, J. Zhang, P. L. F. Hemment, A. F. Willoughby, P. Ward, and P. Ashburn, "Effect of fluorine implantation dose on boron thermal diffusion in silicon," *J. Appl. Phys.*, vol. 96, pp. 4114–4121, 2004.

[9] H. A. W. El Mubarek, M. Karunaratne, J. M. Bonar, G. D. Dilliway, Y. Wang, P. L. F. Hemment, A. F. Willoughby, and P. Ashburn, "Effect of Fluorine implantation dose on boron transient enhanced diffusion and boron thermal diffusion in $Si_{1-x}Ge_x$," *IEEE Trans. Electron Devices*, vol. 52, no. 4, pp. 518–526, Apr. 2005.

[10] T. S. Shano, R. Kim, T. Hirose, Y. Furuta, H. Tsuji, M. Furuhashi, and K. Taniguchi, "Realization of ultrashallow junction: Suppressed boron diffusion and activation by optimized fluorine co-implantation," in *IEDM Tech. Dig.*, 2001, pp. 37.4.1–37.4.4.

[11] G. Impellizzeri, J. H. R. dos Santos, S. Mirabella, F. Priolo, E. Napolitani, and A. Carnera, "Role of fluorine in suppressing boron transient enhanced diffusion in preamorphized Si," *Appl. Phys. Lett.*, vol. 84, pp. 1862–1864, 2004.

[12] N. E. B. Cowern, B. Colombeau, J. Benson, A. J. Smith, W. Lerch, S. Paul, T. Graf, F. Cristiano, X. Hebras, and D. Bolze, "Mechanisms of B deactivation control by F co-implantation," *Appl. Phys. Lett.*, vol. 86, pp. 2055–2057, 2005.

[13] K. Liu, J. Wu, J. Chen, and A. Jain, "Fluorine-assisted super halo for sub50 nm transistors," *IEEE Electron Device Lett.*, vol. 24, no. 2, pp. 180–182, Feb. 2003.

[14] H. Fukutome, Y. Momiyama, H. Nakao, T. Aoyama, and H. Arimoto, "Fluorine implantation impact in extension region on the electrical performance of sub50 nm p-MOSFETs," in *IEDM Tech. Dig.*, 2003, pp. 485–488.

[15] P. M. Fahey, P. B. Griffin, and J. D. Plummer, "Point defects and dopant diffusion in silicon," *Rev. Mod. Phys.*, vol. 61, p. 289, 1989.

[16] G. R. Nash, J. F. W. Schiz, C. D. Marsh, P. Ashburn, and G. R. Booker, "Activation energy for fluorine transport in amorphous silicon," *Appl. Phys. Lett.*, vol. 75, pp. 3671–3673, 1999.

[17] K. S. Jones, S. Prussin, and E. R. Weber, "A systematic analysis of defects in ion implanted silicon," *Appl. Phys. A*, vol. 45, pp. 1–34, 1988.

[18] G. Impellizzeri, "Fluorine enriched silicon: Properties and advantages," Ph.D. dissertation, Univ. Catania, Sicily, Italy, 2004.

[19] N. E. B. Cowern, M. Jaraiz, F. Cristiano, A. Claverlie, and G. Mannino, "Fundamental diffusion issues for deep-submicron device processing," in *IEDM Tech. Dig.*, 1999, pp. 333–336.

[20] I. Avci, M. E. Law, E. Kuryliw, A. F. Saavedra, and K. S. Jones, "Modeling extended defect ($\{311\}$ and dislocation) nucleation and evolution in silicon," *J. Appl. Phys.*, vol. 95, no. 5, pp. 2452–2460, 2003.

[21] R. B. Fair, *Impurity Doping*, F. F. Y. Wang, Ed. Amsterdam, The Netherlands: North Holland, 1981, ch. 7, pp. 315–442.

M. N. Kham, photograph and biography not available at the time of publication.

H. A. W. El Mubarek received the B.Eng. and Ph.D. degrees in electronic engineering from the University of Southampton, Southampton, U.K. in 1999 and 2004, respectively.

Since then she has been working on several research areas including $Si_{1-x}Ge_x$ and $Si_{1-x-y}Ge_xC_y$ HBTs on bulk, SOI and SSOI substrates and has over 20 publications. She is currently a Research Assistant at the University of Southampton in an EPSRC-funded collaborative project between the University of Southampton, University of Surrey, Imperial College, London, Liverpool University, and Queens University, Belfast, Ireland.

J. M. Bonar received the B.A. degree in physics from Reed College, Portland, OR, the M.Sc. degree in materials science from Stevens Institute of Technology, Hoboken, NJ and the Ph.D. degree from the Department of Electronics and Computer Science, University of Southampton, U.K. for research in process development in LPCVD growth.

Her research interests include LPCVD growth and structural characterization of Si and SiGe for devices and diffusion in SiGe. She has over 60 publications in these and related fields.

Peter Ashburn (M'98) was born in Rotherham, U.K., in 1950. He received the B.Sc. degree in electrical and electronic engineering and the Ph.D. degree in experimental and theoretical study of radiation damage in silicon p-n junctions from the University of Leeds, U.K., in 1971 and 1974, respectively.

In 1974, he joined the Technical Staff of Philips Research Laboratories and worked initially on ion implanted integrated circuit bipolar transistors, and then on electron lithography for submicrometer integrated circuits. In 1978, he joined the Academic Staff of the Department of Electronics and Computer Science, University of Southampton, U.K., as a Lecturer, and currently is the holder of a Personal Chair in microelectronics. Since taking up a post at Southampton University, he has worked on polysilicon emitter bipolar transistors, high-speed bipolar and BiCMOS technologies, gate delay expressions for bipolar circuits, and the effects of fluorine in polysilicon emitters. His current research interests include SiGe HBTs, SiGeC and its device applications and vertical MOS transistors for application in sub100-nm CMOS technology. He has authored and coauthored 200 papers in the technical literature, given many invited papers on polysilicon emitters, SiGe HBTs, and vertical MOSFETs and has authored books on the design and realization of bipolar transistors in 1988 and on silicon germanium HBTs in 2003.

P. Ward, photograph and biography not available at the time of publication.

L. Fiore, photograph and biography not available at the time of publication.

R. Petralia, photograph and biography not available at the time of publication.

C. Alemanni, photograph and biography not available at the time of publication.

A. Messina, photograph and biography not available at the time of publication.